Supporting Information

Synthesis of penta- and hexa(3,4-thienylene): Size-dependent structural properties of cyclic oligothiophenes

Mai Nagase,[a,b] Sachiko Nakano,[a] and Yasutomo Segawa*[a,b]

[a] *Institute for Molecular Science, Myodaiji, Okazaki, 444-8787, Japan*
[b] *The Graduate University for Advanced Studies, SOKENDAI, Myodaiji, Okazaki, 444-8787, Japan*

E-mail: segawa@ims.ac.jp

Table of Contents

1. Experimental Section

General

Unless otherwise noted, all materials were obtained from commercial suppliers and used without further purification. Tetrahydrofuran (THF) and toluene for reactions were purified by passing through a solvent purification system (Glass Contour). All reactions were performed with dry solvents under an atmosphere of nitrogen in dried glassware with standard vacuum-line techniques. Work-up and purification procedures were carried out with reagent-grade solvents under air. 3,4-Bis(4,4,5,5-tetramethyl-1,3,2-dioxaborolan-2-yl)thiophene (**1**),[S1] 4,4'-dibromo-3,3'-bithiophene (**3**)[S2] and tetra(3,4-thienylene) (**4T**)[S3] were synthesized according to reported procedure.

Analytical thin-layer chromatography (TLC) was performed using E. Merck silica gel 60 F254 precoated plates (0.25 mm). The developed chromatograms were analyzed by UV lamp (254 or 365 nm). Silica gel column chromatography was performed with KANTO Silica Gel 60N (spherical, neutral, 40-100 μm) or Biotage Isolera® equipped with Biotage® Sfär Silica D Duo 60 μm columns. Preparative recycling gel permeation chromatography (GPC) was performed with a YMC LC-forte/R instrument equipped with JAIGEL-1HH (20 mm I.D. × 600 mm) and JAIGEL-2HH columns (20 mm I.D. × 600 mm) using chloroform ($CHCl_3$) as an eluent. The high-resolution mass spectra (HRMS) were obtained from a Bruker Daltonics maXis (ESI-TOF MS) or a Bruker Daltonics microflex LRF (MALDI-TOF MS) with 7,7,8,8-tetracyanoquinodimethane (TCNQ) as matrix for **4**, **5T**, **5** and **6T**, and silver trifluoroacetate (AgTFA) as cationizing agent for **4** and **5**. Melting points were measured on a MPA100 Optimelt automated melting point system. Nuclear magnetic resonance (NMR) spectra were recorded on a JEOL JNM-ECS400 (^{1}H 400 MHz, ^{13}C 100 MHz) spectrometer. Chemical shifts for ^{1}H NMR are expressed in parts per million (ppm) relative to $CHCl_3$ (δ 7.26 ppm), $CHDCl_2$ (δ 5.32 ppm) or C_2HDCl_4 (δ 5.98 ppm). Chemical shifts for ^{13}C NMR are expressed in ppm relative to $CDCl_3$ (δ 77.16 ppm) or CD_2Cl_2 (δ 53.84 ppm). Data are reported as follows: chemical shift, multiplicity (s = singlet, d = doublet, br = broad signal), coupling constant (Hz), and integration.

Synthesis of 4,4''''-dibromo-3,3':4',3'':4'',3''':4''',3''''-quinquethiophene (4)

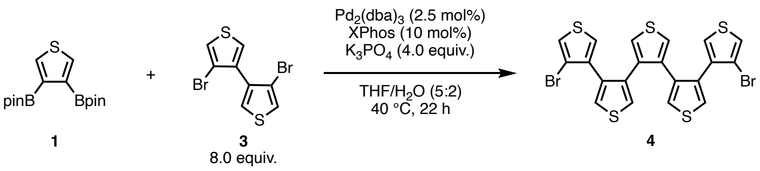

To a 500-mL three-necked round bottom flask containing a magnetic stirring bar were added **1** (2.36 g, 7.02 mmol, 1.0 equiv.), **3** (18.2 g, 56.1 mmol, 8.0 equiv.), 2-dicyclohexylphosphino-2',4',6'-triisopropylbiphenyl (XPhos; 335 mg, 0.700 mmol, 10 mol%), tripotassium phosphate *n*-hydrate ($K_3PO_4 \cdot nH_2O$; 7.45 g, 28.1 mmol, 4.0 equiv.), and tris(dibenzylideneacetone)dipalladium(0) ($Pd_2(dba)_3$; 161 mg, 0.175 mmol, 2.5 mol%). The flask was then evacuated and backfilled with nitrogen three times, and THF (110 mL) and degassed water (45.0 mL) were then added into the flask. The reaction mixture was stirred at 40 °C for 22 h. After quenching the reaction mixture by saturated aqueous ammonium chloride solution, the mixture was extracted with ethyl acetate, washed with water and brine, dried over Na_2SO_4, and then evaporated *in vacuo*. The crude residue was purified by short-path silica gel with dry loading (eluent: hexane, then $CHCl_3$), then silica gel column chromatography (eluent: hexane/$CHCl_3$ = 100:0 to 90:10) to afford **4** as an opaque white solid (2.91 g, 73%).

^{1}H NMR (400 MHz, $CDCl_3$): δ 7.25 (d, J = 3.4 Hz, 2H), 7.11 (d, J = 3.5 Hz, 2H), 7.06 (s, 2H), 6.67 (d, J = 3.4 Hz, 2H), 6.49 (d, J = 3.5 Hz, 2H); ^{13}C NMR (100 MHz, $CDCl_3$): δ 136.8 (4°), 136.7 (4°), 136.5 (4°), 133.8 (4°), 125.0 (CH), 124.7 (CH), 123.7 (CH), 123.1 (CH), 122.7 (CH), 112.1 (4°); HRMS (MALDI-TOF MS) *m/z* calcd for $C_{20}H_{10}Br_2S_5$ $[M+Ag]^+$: 674.680, found: 674.679; mp: 159.1–161.8 °C.

Synthesis of penta(3,4-thienylene) (5T)

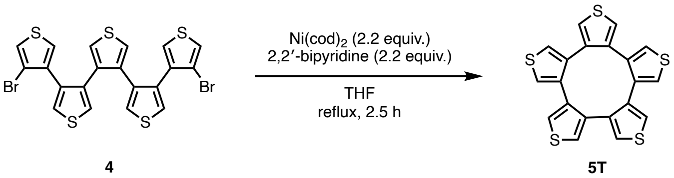

To a 1-L three-necked flask containing a magnetic stirring bar were added **4** (509 mg, 0.892 mmol, 1.0 equiv.) and 2,2′-bipyridine (306 mg, 1.96 mmol, 2.2 equiv.). The flask was then evacuated and backfilled with nitrogen three times, and THF (440 mL) and bis(1,5-cyclooctadiene)nickel(0) (Ni(cod)$_2$; 540 mg, 1.96 mmol, 2.2 equiv.) were then added into the flask. The reaction mixture was refluxed for 2.5 h. After cooling the mixture to room temperature, the reaction mixture was passed through short-path silica gel with CHCl$_3$. The solution was concentrated and the obtained crude residue was purified by silica gel column chromatography (eluent: hexane/CHCl$_3$ = 100:0 to 50:50) to afford **5T** (131 mg, 36%). Single crystals of **5T** suitable for X-ray crystallography were obtained from a hexane/CHCl$_3$ solution.

^{1}H NMR (400 MHz, CD$_2$Cl$_2$, r.t.) δ 7.01 (s, 10H); ^{1}H NMR (400 MHz, CDCl$_3$, r.t.) δ 6.99 (s, 10H); ^{1}H NMR (400 MHz, CD$_2$Cl$_2$, –90 °C) δ 7.01 (s, 10H); ^{13}C NMR (100 MHz, CDCl$_3$) δ 137.6 (4°), 124.6 (CH); HRMS (MALDI-TOF MS) *m/z* calcd for $C_{20}H_{10}S_5$ $[M]^+$: 409.938, found: 409.935; mp: 286.4–289.4 °C (dec.).

Synthesis of 4,4'-bis(4,4,5,5-tetramethyl-1,3,2-dioxaborolan-2-yl)-3,3'-bithiophene (2)

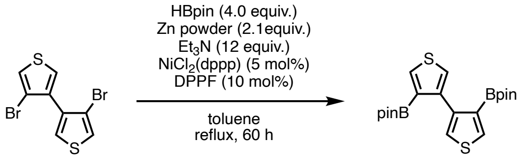

3 **2**

To a 100-mL two-necked flask containing a magnetic stirring bar were added **3** (3.24 g, 10.0 mmol, 1.0 equiv.), 1,3-bis(diphenylphosphino)propane]dichloronickel(II) ($NiCl_2$(dppp); 271 mg, 0.500 mmol, 5.0 mol%), 1,1′-bis(diphenylphosphino)ferrocene (DPPF; 554 mg, 1.00 mmol, 10 mol%), and Zn powder (1.34 g, 20.5 mmol, 2.1 equiv.). The flask was then evacuated and backfilled with nitrogen three times, and toluene (20.0 mL) and degassed triethylamine (Et_3N; 17.0 mL, 122 mmol, 12 equiv.) were added via syringe. Then, 4,4,5,5-tetramethyl-1,3,2-dioxaborolane (HBpin; 5.80 mL, 40.0 mmol, 4.0 equiv.) was added dropwise via syringe, and the resulting solution was refluxed for 60 h. After cooling the mixture to room temperature, the reaction mixture was passed through short-path silica gel with $CHCl_3$. The product was extracted with $CHCl_3$ using a saturated aqueous ammonium chloride solution, washed with water and brine, dried over Na_2SO_4, and then evaporated *in vacuo*. The solution was concentrated and the obtained crude residue was purified by silica gel column chromatography (eluent: hexane/$CHCl_3$ = 90:10 to 0:100) to afford **2** (2.02 g, 48%). Single crystals of **2** suitable for X-ray crystallography were obtained by slow evaporation of hexane solution.

^{1}H NMR (400 MHz, $CDCl_3$) δ 7.81 (d, J = 3.1 Hz, 2H), 7.28 (d, J = 3.1 Hz, 2H), 1.22 (s, 24H); ^{13}C NMR (100 MHz, $CDCl_3$) δ 142.3 (4°), 136.6 (br, 4°), 135.5 (CH), 124.2 (CH), 83.4 (4°), 24.8 (CH_3); HRMS (ESI-TOF MS) *m/z* calcd for $C_{20}H_{28}B_2O_4S_2$ $[M+H]^+$: 419.170, found: 419.171; mp: 116.9–118.6 °C (dec.).

Synthesis of 4,4'''''-dibromo-3,3':4',3'':4'',3''':4''',3'''':4'''',3'''''-sexithiophene (5)

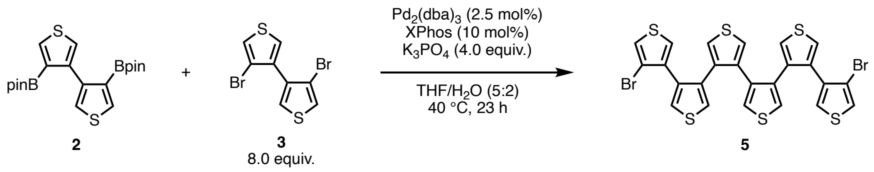

To a 200-mL two-necked round bottom flask containing a magnetic stirring bar were added **2** (1.25 g, 3.00 mmol), **3** (7.78 g, 24.0 mmol, 8.0 equiv.), XPhos (143 mg, 0.300 mmol, 10 mol%), $K_3PO_4 \cdot nH_2O$ (3.18 g, 12.0 mmol, 4.0 equiv.), and $Pd_2(dba)_3$ (68.7 mg, 0.0750 mmol, 2.5 mol%). The flask was then evacuated and backfilled with nitrogen three times, and THF (45 mL) and degassed water (18 mL) were then added into the flask. The reaction mixture was stirred at 40 °C for 23 h. After quenching the reaction mixture by saturated aqueous ammonium chloride solution, the mixture was extracted with ethyl acetate three times, washed with water and brine, dried over Na_2SO_4, and then evaporated *in vacuo*. The crude residue was purified by short-path silica gel with dry loading (eluent: hexane, then $CHCl_3$), then silica gel column chromatography (eluent: hexane/$CHCl_3$ = 100:10 to 80:20) to afford **5** as an opaque white solid (1.01 g, 52%).

^{1}H NMR (400 MHz, CD_2Cl_2) δ 7.27 (d, J = 3.4 Hz, 2H), 7.13 (d, J = 3.5 Hz, 2H), 6.97 (d, J = 3.4 Hz, 2H), 6.68 (d, J = 3.4 Hz, 2H), 6.56 (d, J = 3.4 Hz, 2H), 6.35 (d, J = 3.5 Hz, 2H); ^{13}C NMR (100 MHz, CD_2Cl_2) δ 137.5 (4°), 137.0 (4°), 136.3 (4°), 136.0 (4°), 134.0 (4°), 125.1 (CH), 124.3 (CH), 123.9 (CH), 123.5 (CH), 123.2 (CH), 112.0 (4°); HRMS (MALDI-TOF MS) *m/z* calcd for $C_{24}H_{12}Br_2S_6$ $[M+Ag]^+$: 758.666, found: 758.664; mp: 184.7–185.9 °C.

Synthesis of hexa(3,4-thienylene) (6T)

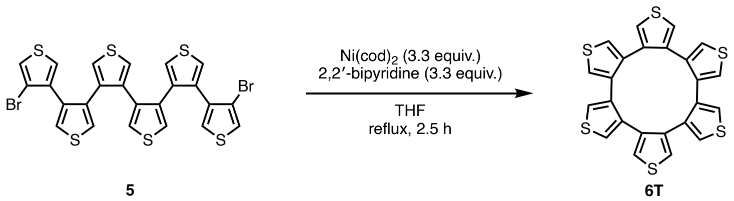

After a 500-mL three-necked flask containing a magnetic stirring bar was evacuated and backfilled with nitrogen three times, **5** (281 mg, 0.430 mmol), 2,2'-bipyridine (222 mg, 1.42 mmol, 3.3 equiv.), THF (251 mL), and Ni(cod)$_2$ (390 mg, 1.42 mmol, 3.3 equiv.) were added into the flask. The reaction mixture was refluxed for 2.5 h. After cooling the mixture to room temperature, the reaction mixture was passed through short-path silica gel with $CHCl_3$ and THF. The solution was concentrated and the obtained crude residue was purified by silica gel column chromatography (eluent: hexane/$CHCl_3$ = 90:10 to 50:50) and GPC (eluent: $CHCl_3$) to afford **6T** (3.1 mg, 1.5%). Single crystals of **6T** suitable for X-ray crystallography were obtained from a pentane/THF solution.

^{1}H NMR (400 MHz, CD_2Cl_2, r.t.) δ 7.29 (s, 4H), 6.91 (d, J = 3.2 Hz, 4H), 6.48 (d, J = 3.2 Hz, 4H); ^{1}H NMR (400 MHz, $C_2D_2Cl_4$, 140 °C) δ 7.32 (s, 4H), 6.92 (d, J = 3.4 Hz, 4H), 6.53 (d, J = 3.4 Hz, 4H); ^{13}C NMR (100 MHz, $CDCl_3$) δ 138.9 (4°), 135.7 (4°), 134.2 (4°), 126.1 (CH), 123.3 (CH), 122.7 (CH); HRMS (MALDI-TOF MS) *m/z* calcd for $C_{24}H_{12}S_6$ $[M]^+$: 491.926, found: 491.923; mp: 284.5–289.0 °C (dec.).

Table S1. Solubility of **5T** and **6T** in diethyl ether, $CHCl_3$, and THF.

	diethyl ether (mg/mL)	$CHCl_3$ (mg/mL)	THF (mg/mL)
5T	0.5	4.4	10.3
6T	0.5	3.0	9.0

2. X-ray Crystallography

Details of the crystal data and a summary of the intensity data collection parameters for **5T**, **2**, and **6T** are listed in Table S2. Suitable crystals were mounted with mineral oil on a MiTeGen MicroMounts and transferred to the goniometer of the kappa goniometer of a RIGAKU XtaLAB Synergy Custom system with equipped with mirror monochromated Mo Kα radiation (λ = 0.71073 Å) and HyPix-6000HEIC detector. Cell parameters were determined and refined, and raw frame data were integrated using CrysAlisPro (Rigaku Oxford Diffraction, 2018). The structures were solved by dual methods using SHELXT[S4] and refined by full-matrix least-squares techniques against F^2 with SHELXL-2018/3[S5] using Olex2 software package.[S6] The intensities were corrected for Lorentz and polarization effects. All non-hydrogen atoms were refined with anisotropic displacement parameters. Hydrogen atoms were placed using AFIX instructions and refined isotropically.

Table S2. Crystallographic data and structure refinement details of **5T**, **2**, and **6T**.

	5T	**2**	**6T**
CCDC No.	2281497	2281496	2281498
formula	$C_{20}H_{10}S_5$	$C_{40}H_{56}B_4O_8S_4$	$C_{24}H_{12}S_6$
fw	410.58	836.32	492.70
T (K)	123(2)	123(2)	123(2)
λ (Å)	0.71073	0.71073	0.71073
cryst syst	monoclinic	triclinic	monoclinic
space group	$I2/a$	P-1	$I2/a$
a (Å)	12.1542(5)	10.9669(3)	13.6292(10)
b (Å)	10.6118(3)	11.1772(2)	12.2216(5)
c (Å)	13.9023(5)	19.4756(7)	14.3297(12)
α (deg)	90	86.670(2)	90
β (deg)	107.303(4)	85.723(2)	117.598(10)
γ (deg)	90	71.102(2)	90
V (Å^3)	1711.94(11)	2250.87(11)	2115.3(3)
Z	4	2	4
D_{calc} (g·cm^{-3})	1.593	1.234	1.547
μ (mm^{-1})	0.677	0.259	0.657
F(000)	840.0	888.0	1008.0
cryst size (mm)	0.15 × 0.1 × 0.05	0.11 × 0.08 × 0.05	0.2 × 0.1 × 0.1
2θ range (deg)	4.914–62.424	4.566–62.96	6.846–59.778
reflns collected	6906	39866	7772
indep reflns/R_{int}	2289 / 0.0259	12381 / 0.0373	2457 / 0.0244
params	114	521	136
GOF on F^2	1.072	1.157	1.030
R_1, wR_2 [I>2$\sigma(I)$]	0.0319, 0.0805	0.0692, 0.1534	0.0407, 0.1036
R_1, wR_2 (all data)	0.0358, 0.0833	0.0947, 0.1617	0.0547, 0.1127

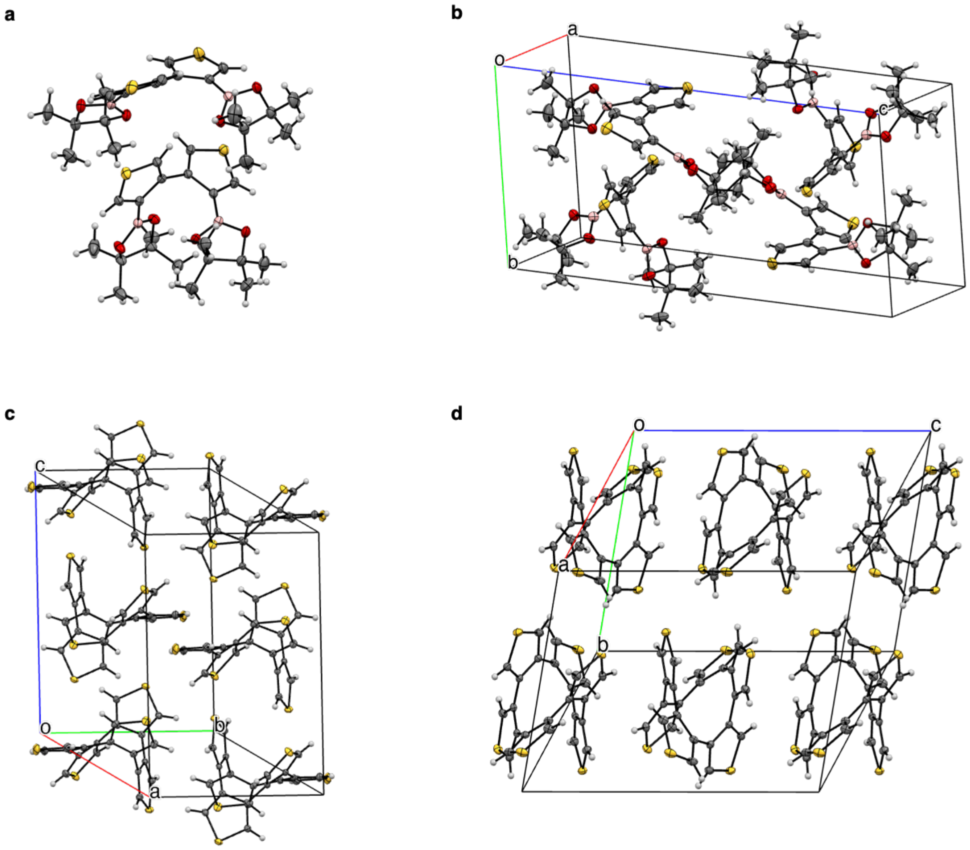

Fig. S1 (a) Molecular structure of **2** with thermal ellipsoids at 50% probability. (b) Packing structure of **2**. (c) Packing structure of **5T**. (d) Packing structure of **6T**.

3. Photophysical Measurement

UV-vis absorption spectra were recorded on a JASCO V-770 spectrometer with a resolution of 0.5 nm. Dilute solutions in spectral-grade dichloromethane in a 1 cm square quartz cell were used for measurements. The longest-wavelength absorption maxima were determined by curve fitting with Gaussian functions.

4. Computational Study

The Gaussian 16 program[S7] running on a NEC LX 110Rh system was used for optimization. Structures were optimized at B3LYP/6-31G(d)[S8,S9] with or without Grimme's D3 type dispersion.[S10] NMR chemical shifts are calculated by GIAO[S11] method. Zero-point energy, enthalpy, and Gibbs free energy at 298.15 K and 1 atm were estimated from the gas-phase studies. Harmonic vibration frequency calculation at the same level was performed to verify all stationary points as local minima (with no imaginary frequency) or transition states (with one imaginary frequency). Cartesian coordinates of optimized structures are included in CartesianCoordinates.xyz file.

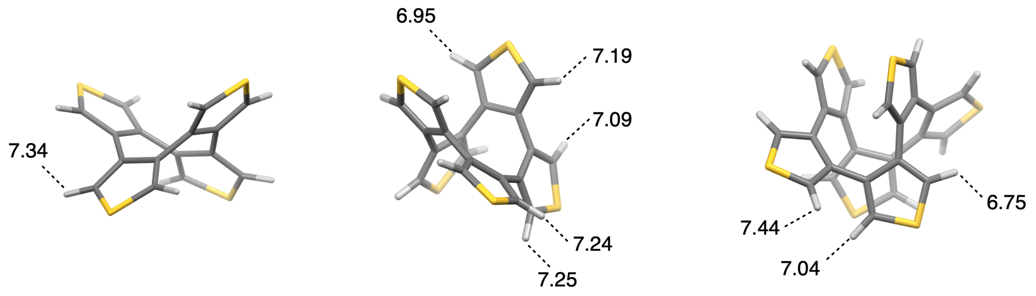

4T **5T** **6T**

Fig. S2 Calculated ^{1}H NMR chemical shifts (ppm) using GIAO B3LYP/6-311+G(2d,p)//B3LYP-D3/6-31G(d) level with tetramethylsilane as a reference (0.00 ppm).

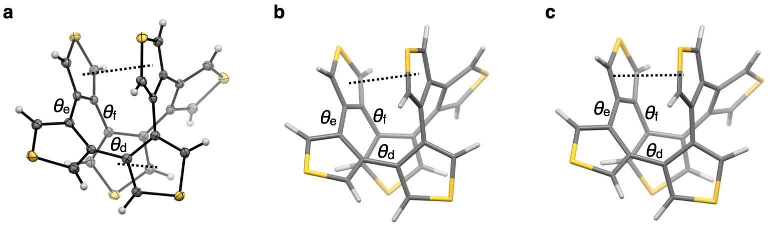

6T$_{\text{X-ray}}$ **6T**(B3LYP) **6T**(B3LYP-D3)

d

	θd (°)	θe (°)	θf (°)	π-π (Å)
6T$_{\text{X-ray}}$	41.8	46.0	124.5	3.40†
6T(B3LYP)	45.1	45.1	120.5	3.59
6T(B3LYP-D3)	44.9	44.9	121.5	3.41

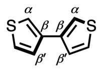

e

	θobs (°)	θcalcd (°)
4T	54.3[S12]	55.8
5T	46.0, 90.8, 87.8	46.0, 85.1, 96.2
6T	41.8, 46.0, 124.5	44.9, 121.5

Fig. S3 Structural parameters of **4T**–**6T**. (a) Structure of **6T** determined by X-ray crystallography. (b) Structure of **6T** optimized at the B3LYP/6-31G(d) level. (c) Structure of **6T** optimized at the B3LYP-D3/6-31G(d) level. (d) Average dihedral angles (*α*-*β*-*β*-*α* and *β*-*β*-*β*-*β*) and π-π distance. †Average of two π-π distances. (e) Average dihedral angles in **4T**–**6T** obtained from the X-ray crystal structures and the structures theoretically optimized at the B3LYP-D3/6-31G(d) level.

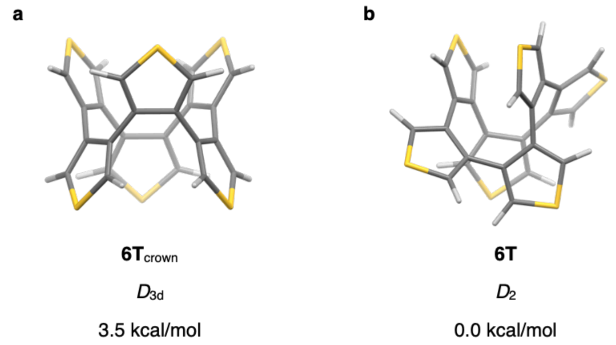

Fig. S4 Relative Gibbs free energy (sum of electronic and thermal free energy) calculated at the B3LYP-D3/6-31G(d) level. (a) D_{3d}-Symmetric structure of **6T**. (b) D_2-Symmetric structure of **6T**.

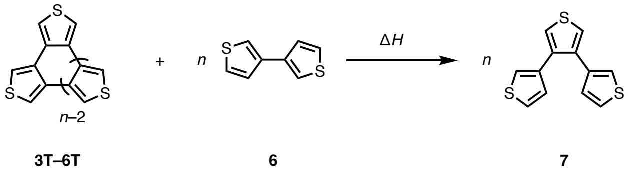

	n	ΔH (kcal·mol^{-1})
3T	3	–1.4
4T	4	4.8
5T	5	19.9
6T	6	1.1

Fig. S5 Homodesmotic reactions to estimate the strain energies of **3T**–**6T** (ΔH, kcal mol^{-1}).

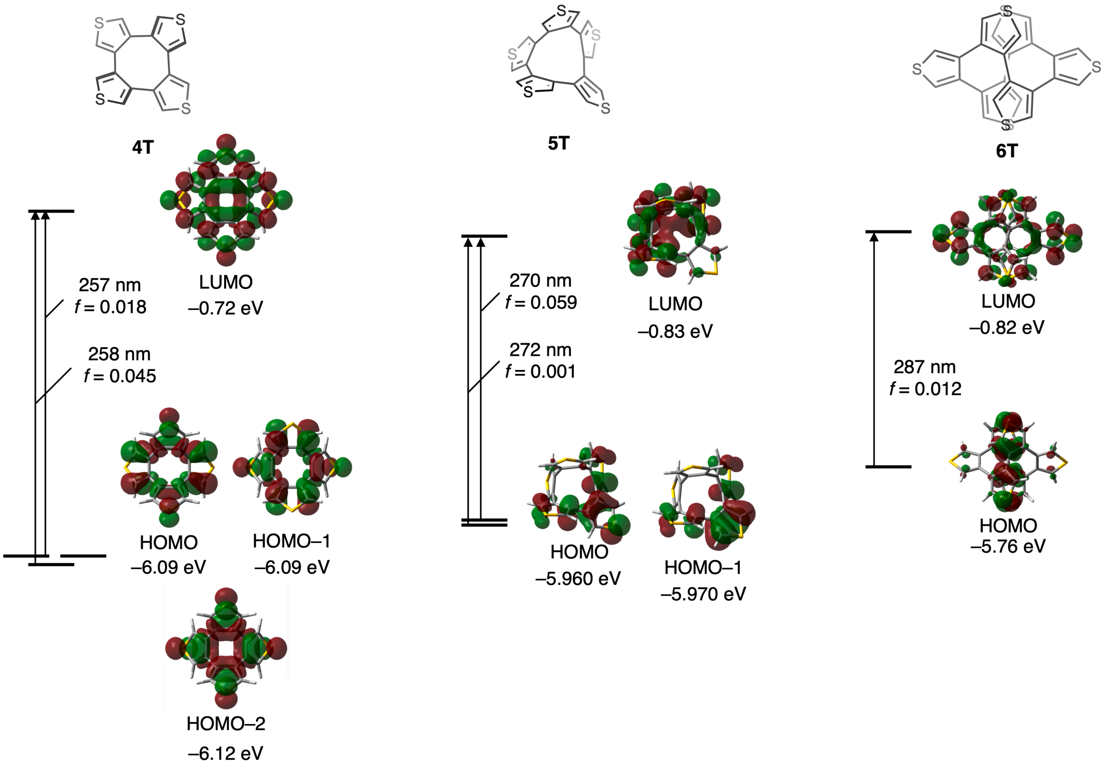

Fig. S6 Frontier molecular orbitals and energy levels of **4T**, **5T**, and **6T** calculated at the B3LYP-D3/6-31G(d) level (isovalue = 0.03). Excitation energies were calculated by TD-DFT calculations at the same level. The *f* values refer to the oscillator strength.

Table S3. Uncorrected and thermal-corrected (298 K) energies of stationary points (Hartree).[a]

	E	$E + ZPE$	H	G
3T	-1655.46266350	-1655.321723	-1655.309549	-1655.359588
4T	-2207.27372822	-2207.085189	-2207.068756	-2207.127373
5T	-2759.07050599	-2758.834552	-2758.813766	-2758.883284
5T$_{\mathbf{TS}}$	-2759.06291372	-2758.827414	-2758.807300	-2758.875348
6T(B3LYP)	-3310.84731729	-3310.563934	-3310.53987	-3310.615717
6T(B3LYP-D3)	-3310.92145750	-3310.637534	-3310.612819	-3310.688461
6T$_{\mathbf{TS}}$	-3310.87496770	-3310.591902	-3310.567571	-3310.646265
6T$_{\mathbf{crown}}$	-3310.90814920	-3310.625340	-3310.599887	-3310.682900
6	-1104.82703489	-1104.712578	-1104.703324	-1104.747193
7	-1656.64784298	-1656.486009	-1656.472413	-1656.527017

[a] E: electronic energy; ZPE: zero-point energy; H (= $E + ZPE + E_{\mathrm{vib}} + E_{\mathrm{rot}} + E_{\mathrm{trans}} + RT$): sum of electronic and thermal enthalpies; G (= $H - TS$): sum of electronic and thermal free energies.

5. References

[S1] K. Kise, F. Chen, K. Kato, T. Tanaka and A. Osuka, *Chem. Lett.*, 2017, **46**, 1319–1322.

[S2] A. Rajca, M. Miyasaka, M. Pink, H. Wang and S. Rajca, *J. Am. Chem. Soc.*, 2004, **126**, 15211–15222.

[S3] S. Zhang, X. Liu, C. Li, L. Li, J. Song, J. Shi, M. Morton, S. Rajca, A. Rajca and H. Wang, *J. Am. Chem. Soc.*, 2016, **138**, 10002–10010.

[S4] G. M. Sheldrick, *Acta Crystallogr.* 2015, **A71**, 3–8.

[S5] G. M. Sheldrick, *Acta Crystallogr.* 2015, **C71**, 3–8.

[S6] O. V. Dolomanov, L. J. Bourhis, R. J. Gildea, J. A. K. Howard and H. Puschmann, *J. Appl. Crystallogr.* 2009, **42**, 339–341.

[S7] M. J. Frisch, G. W. Trucks, H. B. Schlegel, G. E. Scuseria, M. A. Robb, J. R. Cheeseman, G. Scalmani, V. Barone, G. A. Petersson, H. Nakatsuji, X. Li, M. Caricato, A. V. Marenich, J. Bloino, B. G. Janesko, R. Gomperts, B. Mennucci, H. P. Hratchian, J. V. Ortiz, A. F. Izmaylov, J. L. Sonnenberg, D. Williams-Young, F. Ding, F. Lipparini, F. Egidi, J. Goings, B. Peng, A. Petrone, T. Henderson, D. Ranasinghe, V. G. Zakrzewski, J. Gao, N. Rega, G. Zheng, W. Liang, M. Hada, M. Ehara, K. Toyota, R. Fukuda, J. Hasegawa, M. Ishida, T. Nakajima, Y. Honda, O. Kitao, H. Nakai, T. Vreven, K. Throssell, J. A. Montgomery, Jr., J. E. Peralta, F. Ogliaro, M. J. Bearpark, J. J. Heyd, E. N. Brothers, K. N. Kudin, V. N. Staroverov, T. A. Keith, R. Kobayashi, J. Normand, K. Raghavachari, A. P. Rendell, J. C. Burant, S. S. Iyengar, J. Tomasi, M. Cossi, J. M. Millam, M. Klene, C. Adamo, R. Cammi, J. W. Ochterski, R. L. Martin, K. Morokuma, O. Farkas, J. B. Foresman and D. J. Fox, Gaussian 16, Revision B.01, Gaussian, Inc., Wallingford CT, 2016.

[S8] A. D. Becke, *J. Chem. Phys.* 1993, **98**, 5648–5652.

[S9] C. Lee, W. Yang and R. G. Parr, *Phys. Rev. B* 1988, **37**, 785–789.

[S10] S. Grimme, J. Antony, S. Ehrlich and H. Krieg, *J. Chem. Phys.*, 2010, **132**, 154104.

[S11] K. Wolinski, J. F. Hinton and P. Pulay, *J. Am. Chem. Soc.*, 1990, **112**, 8251–8260.

[S12] T. Fujimoto, R. Suizu, H. Yoshikawa and K. Awaga, *Chem. Eur. J.*, 2008, **14**, 6053.

6. ^{1}H NMR, ^{13}C NMR and Mass Spectra of Products

^{1}H NMR spectrum of **4** (400 MHz, $CDCl_3$)

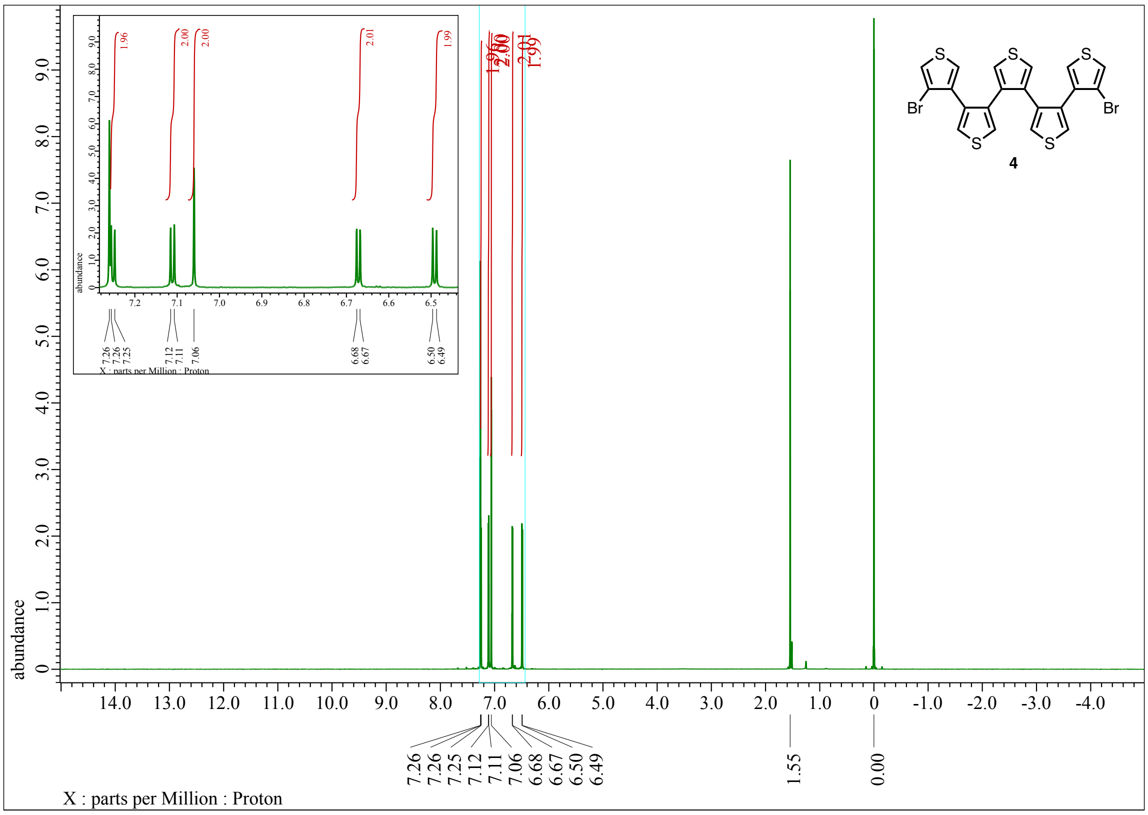

^{13}C NMR spectrum of **4** (100 MHz, $CDCl_3$)

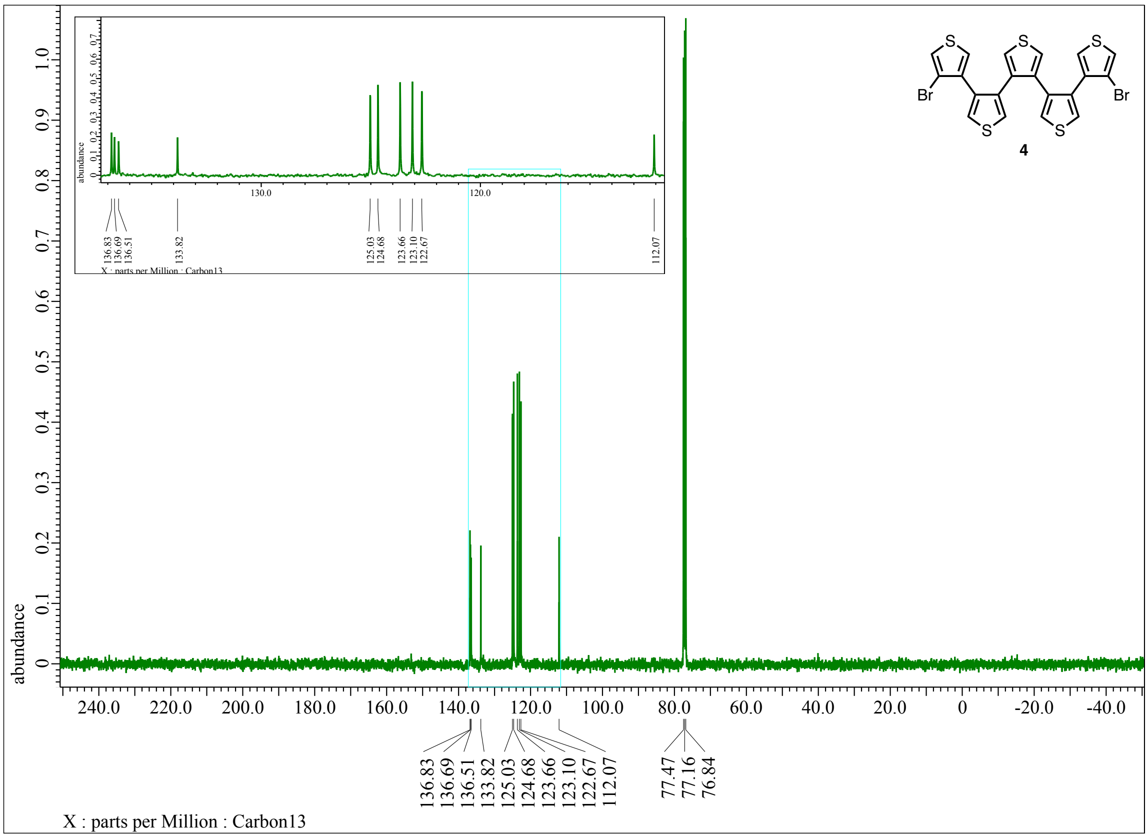

Mass spectrum of **4** (MALDI-TOF MS)

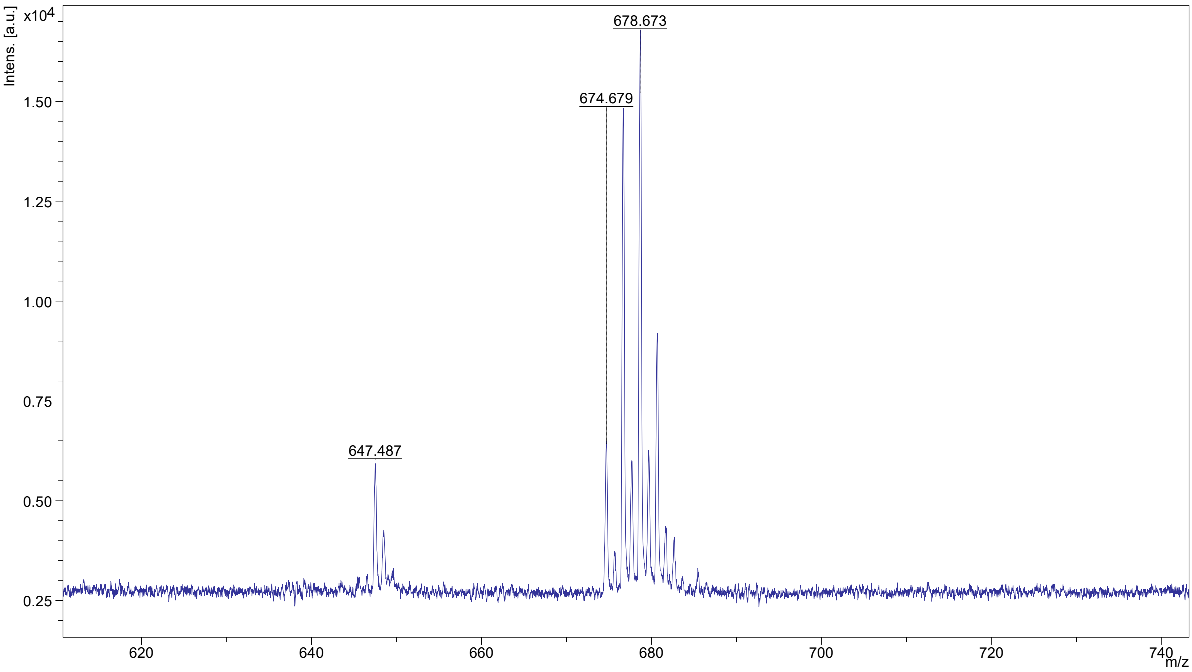

^{1}H NMR spectrum of **5T** (400 MHz, CD_2Cl_2) at room temperature

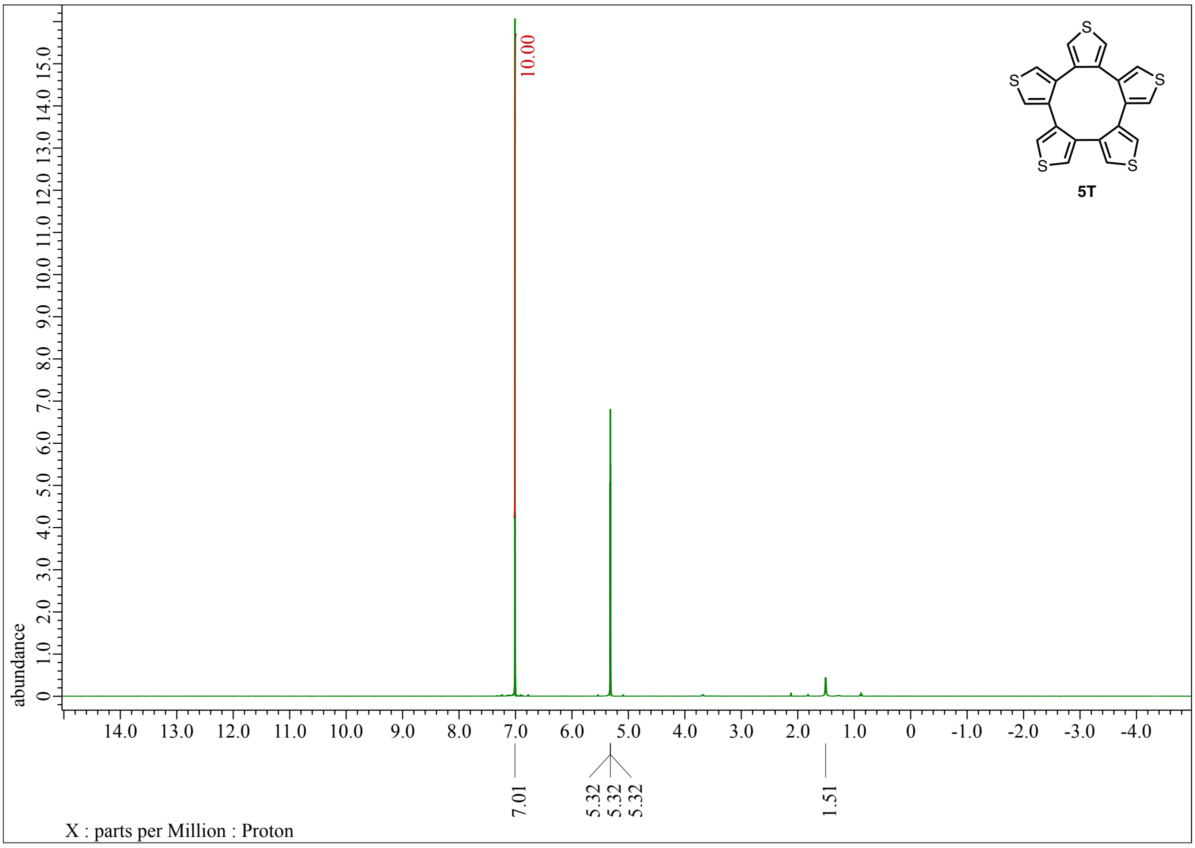

^{1}H NMR spectrum of **5T** (400 MHz, CDCl$_3$) at room temperature

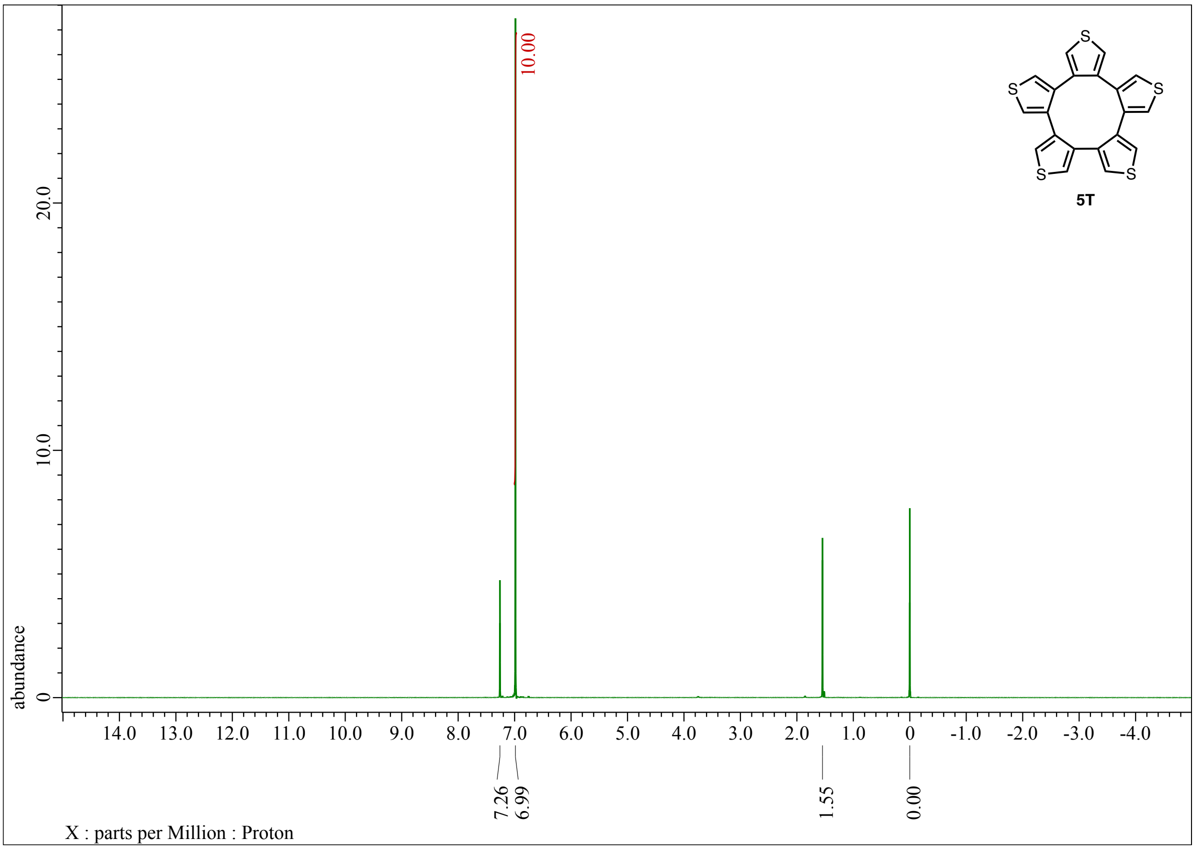

^{1}H NMR spectrum of **5T** (400 MHz, CD$_2$Cl$_2$) at –90 °C

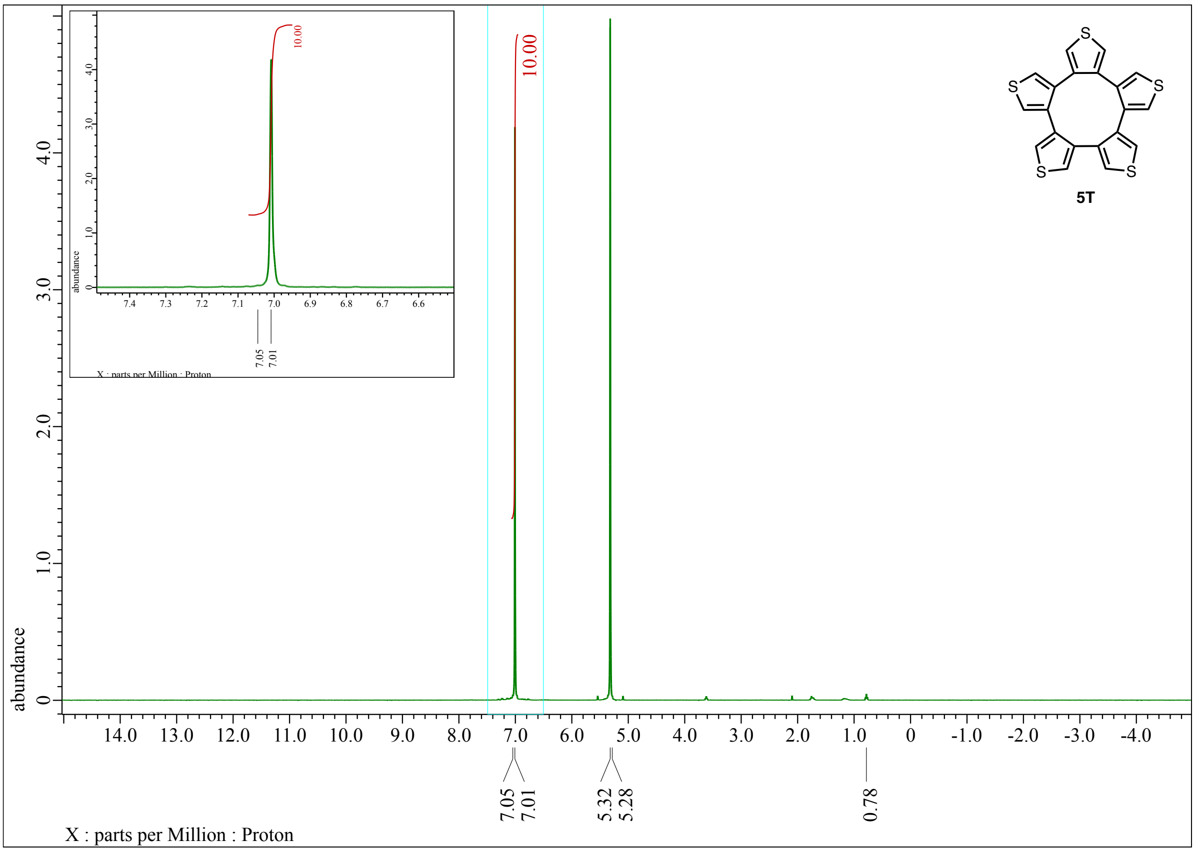

^{13}C NMR spectrum of **5T** (100 MHz, $CDCl_3$)

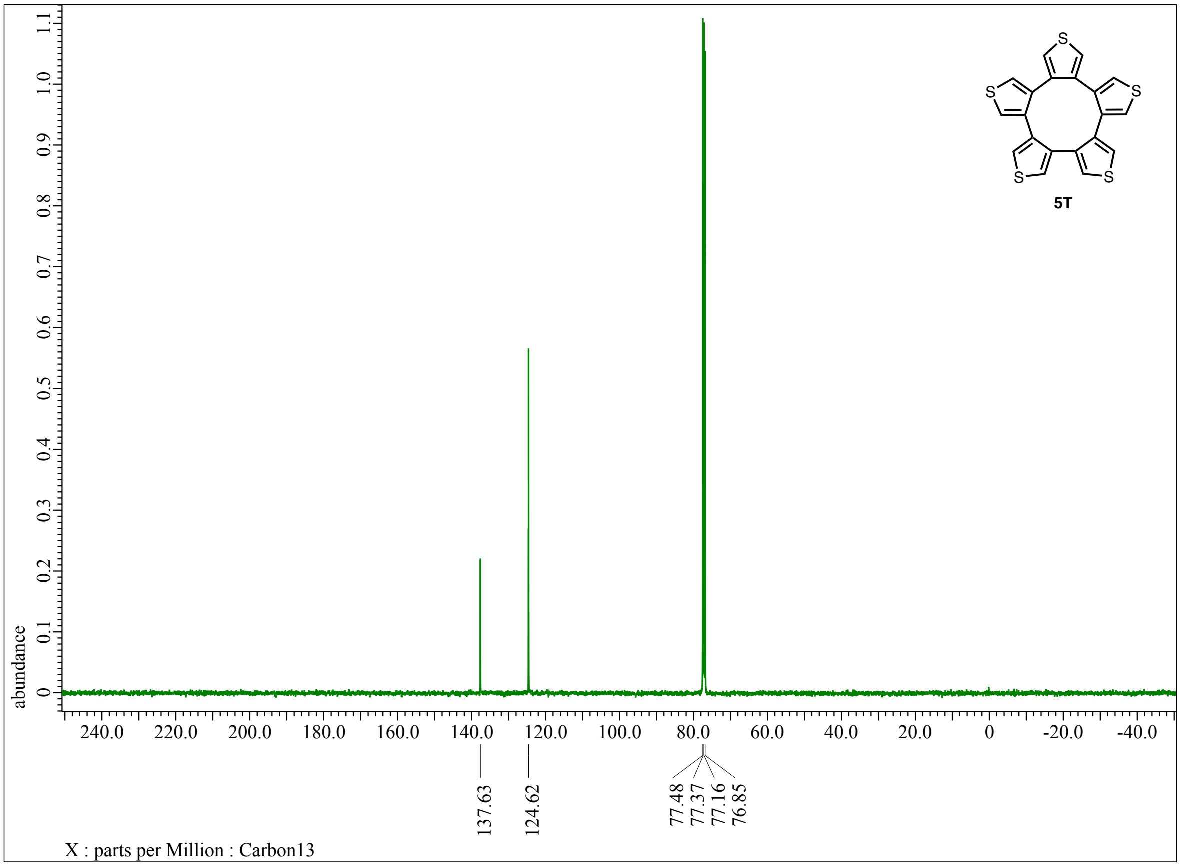

Mass spectrum of **5T** (MALDI-TOF MS)

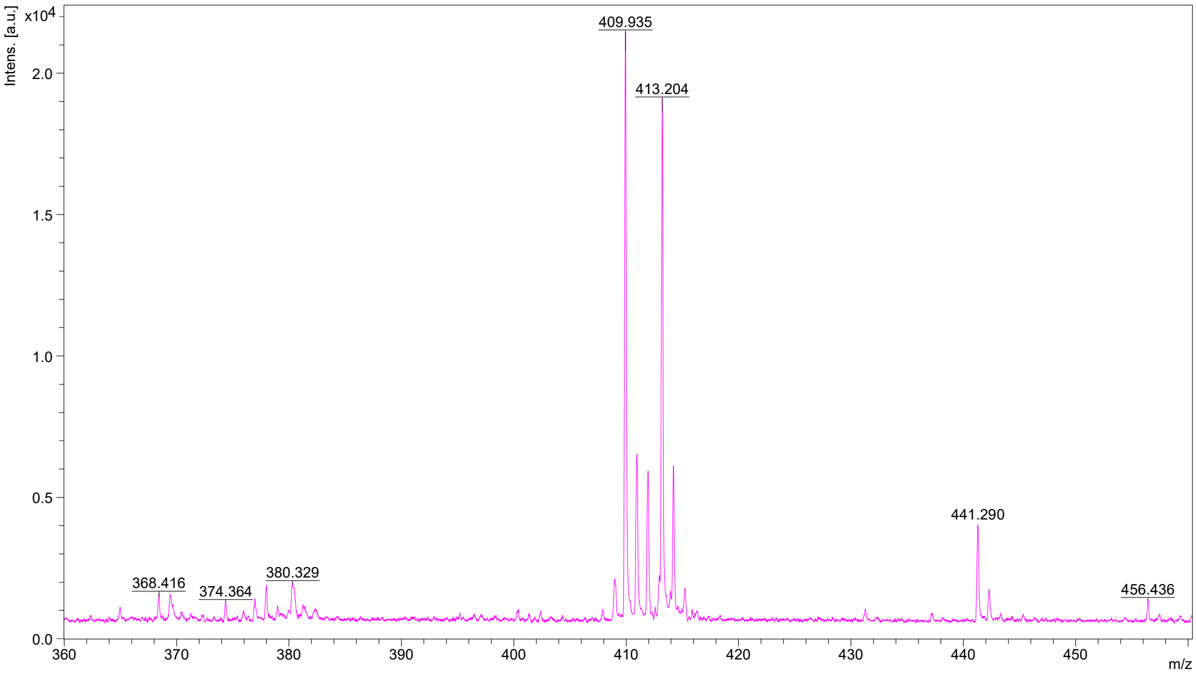

^{1}H NMR spectrum of **2** (400 MHz, $CDCl_3$)

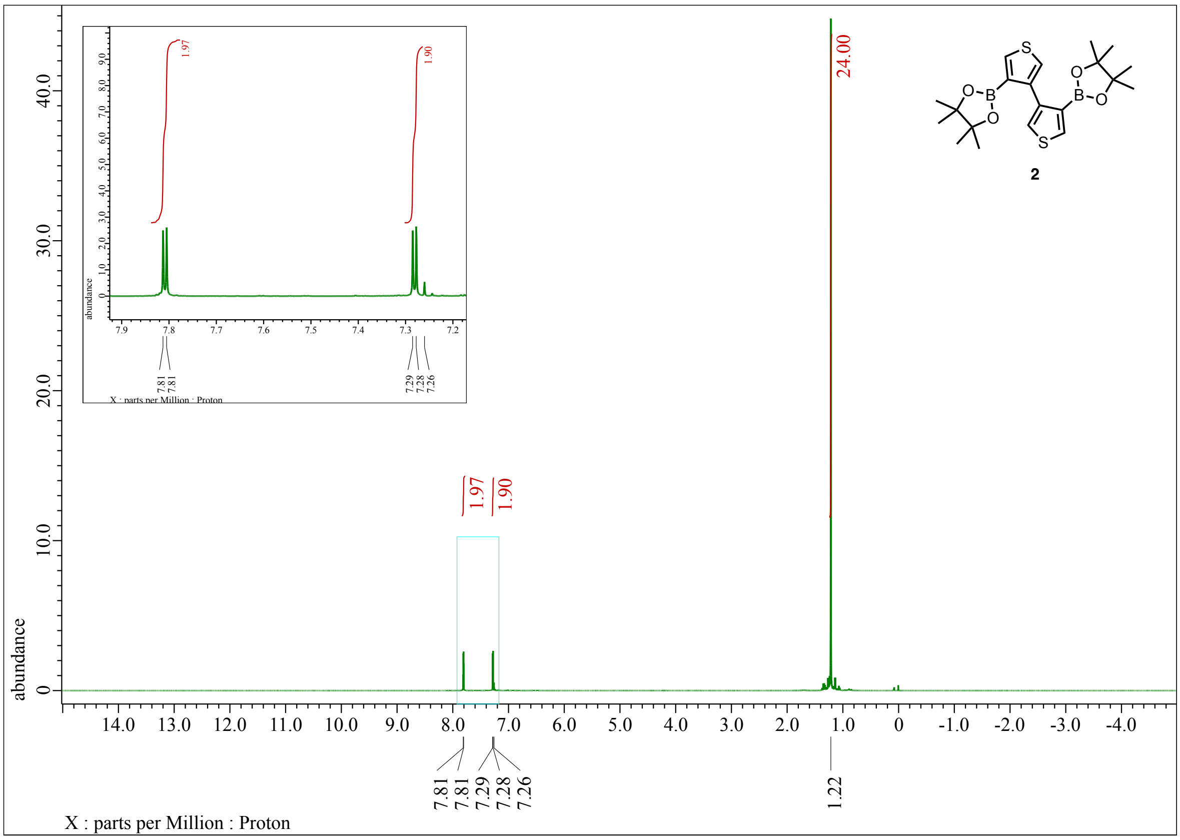

^{13}C NMR spectrum of **2** (100 MHz, $CDCl_3$)

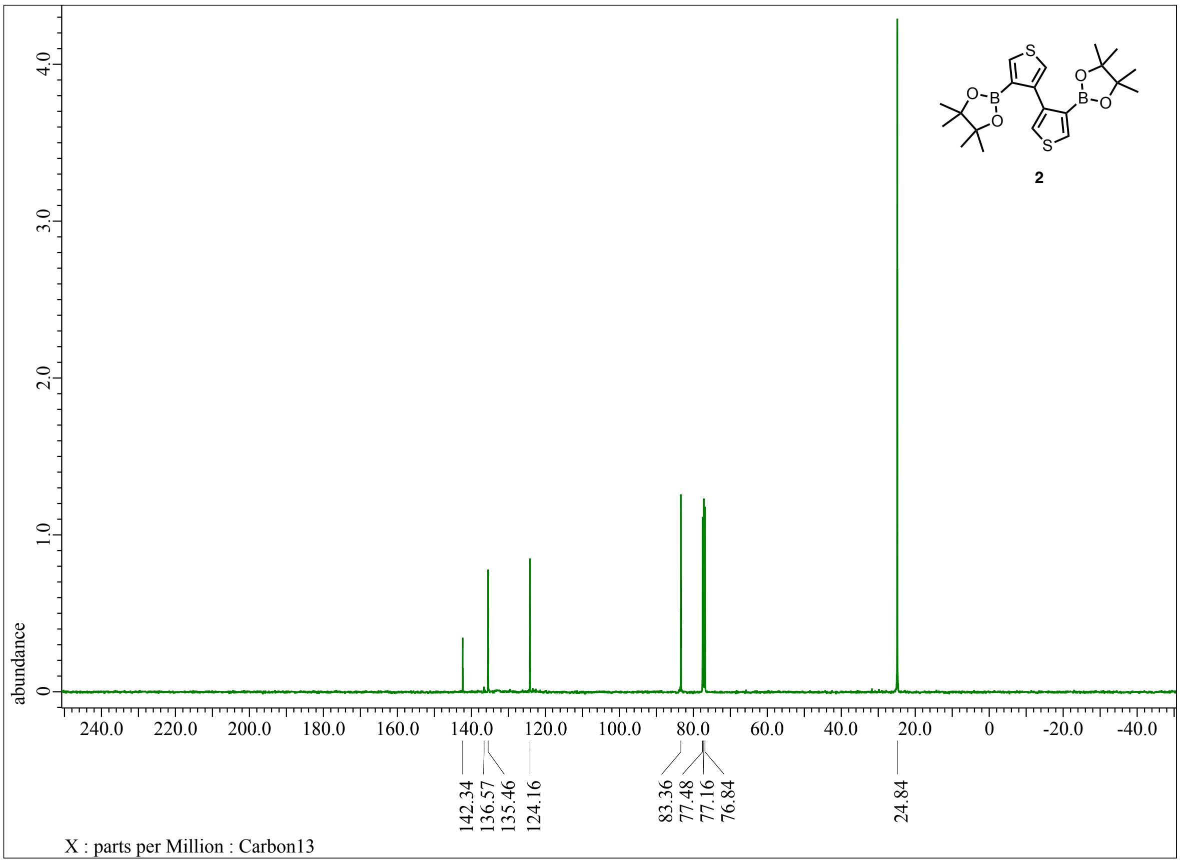

Mass spectrum of **2** (ESI-TOF MS)

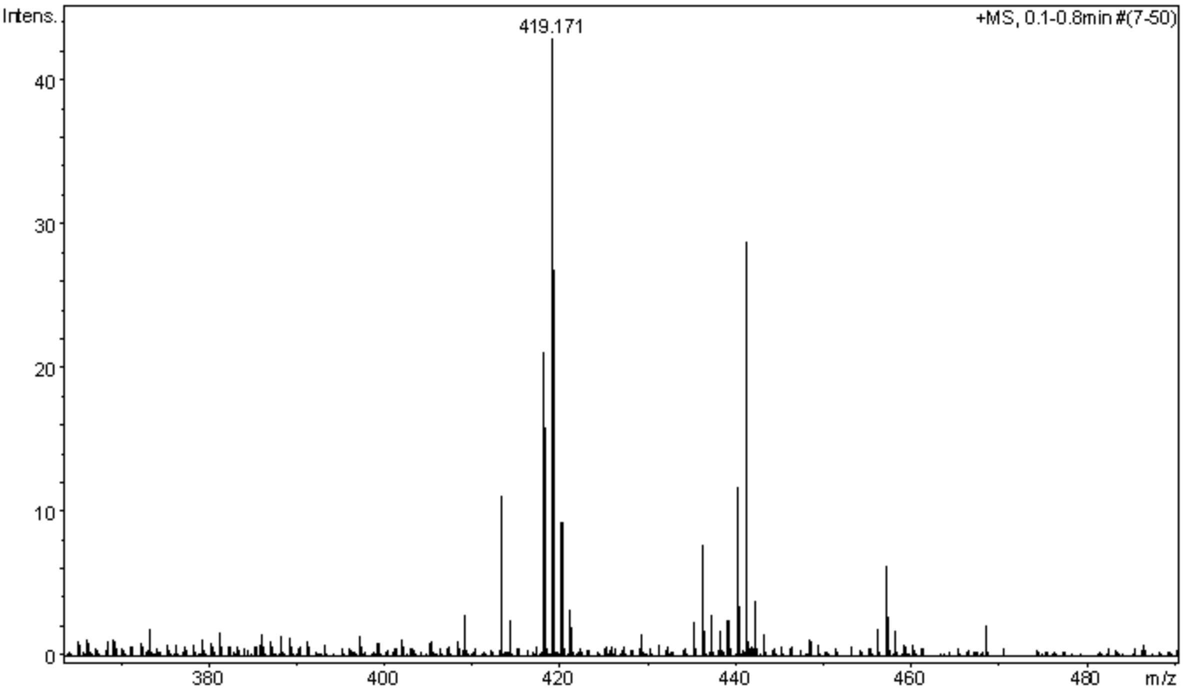

^{1}H NMR spectrum of **5** (400 MHz, CD_2Cl_2)

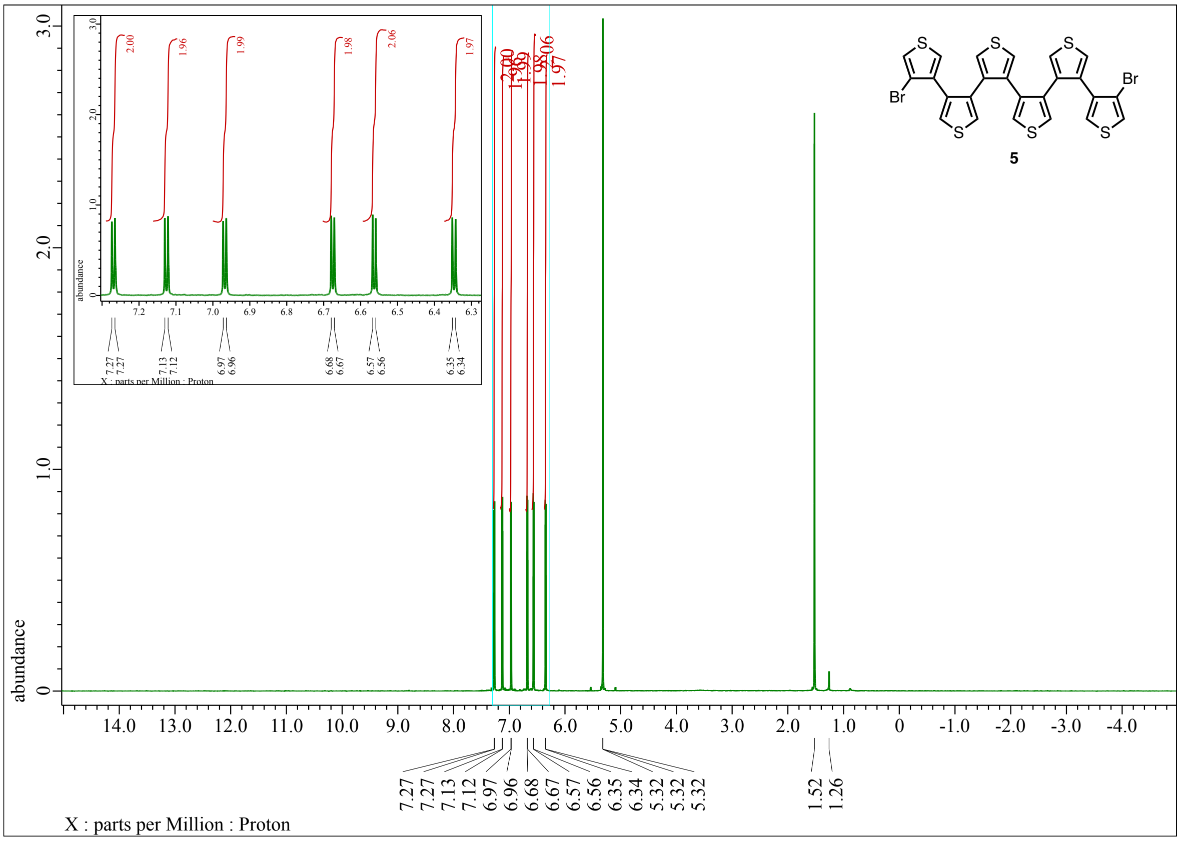

^{13}C NMR spectrum of **5** (100 MHz, CD_2Cl_2)

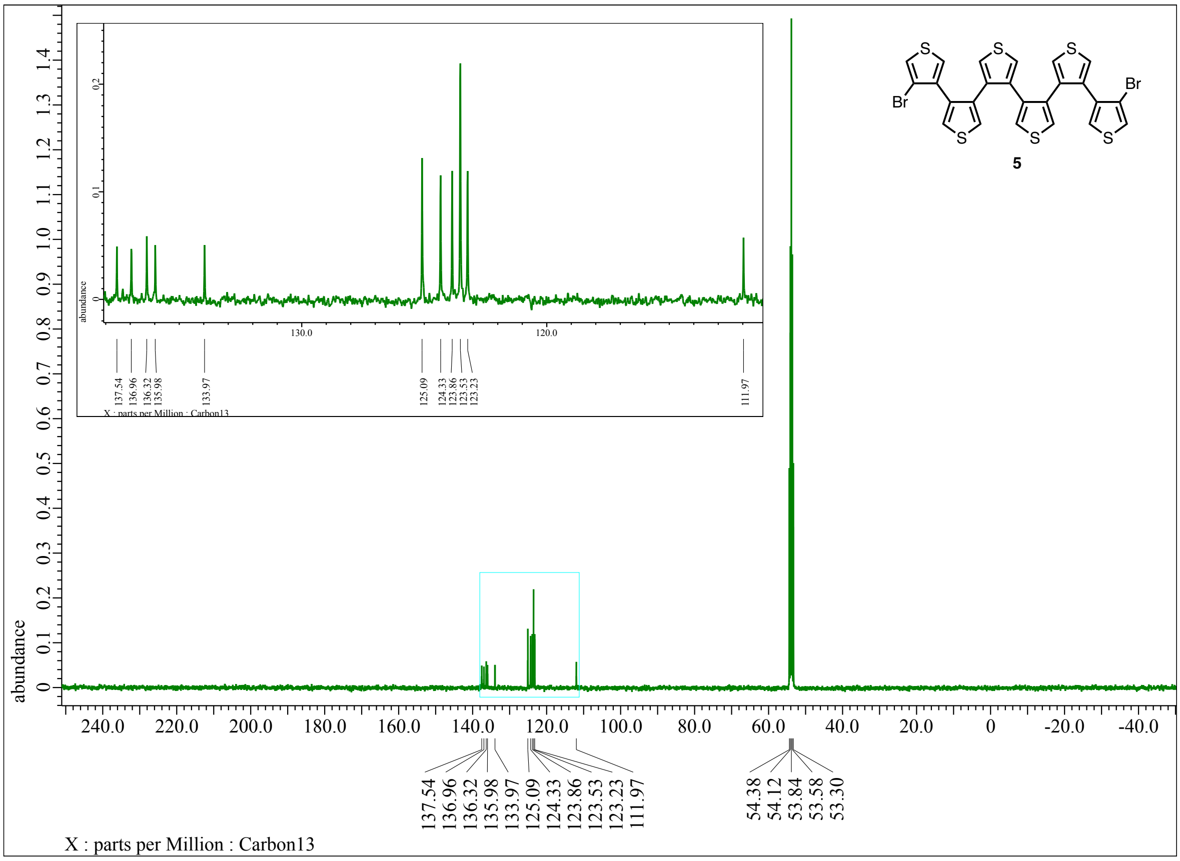

Mass spectrum of **5** (MALDI-TOF MS)

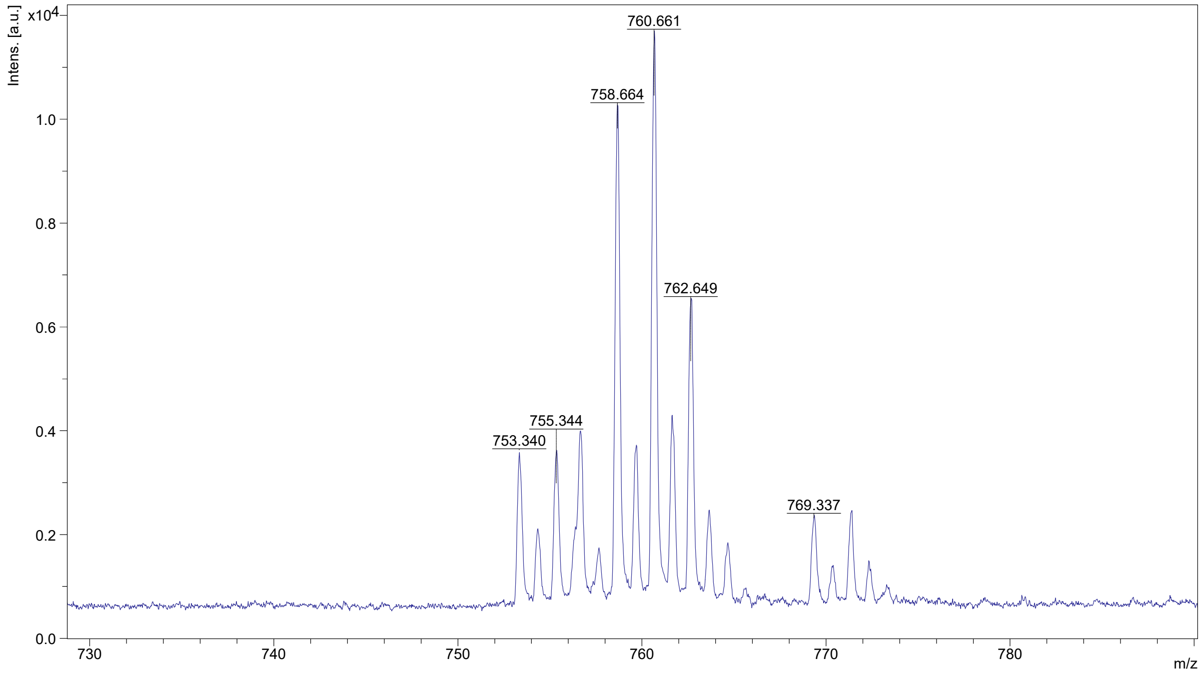

^{1}H NMR spectrum of **6T** (400 MHz, CD_2Cl_2) at room temperature

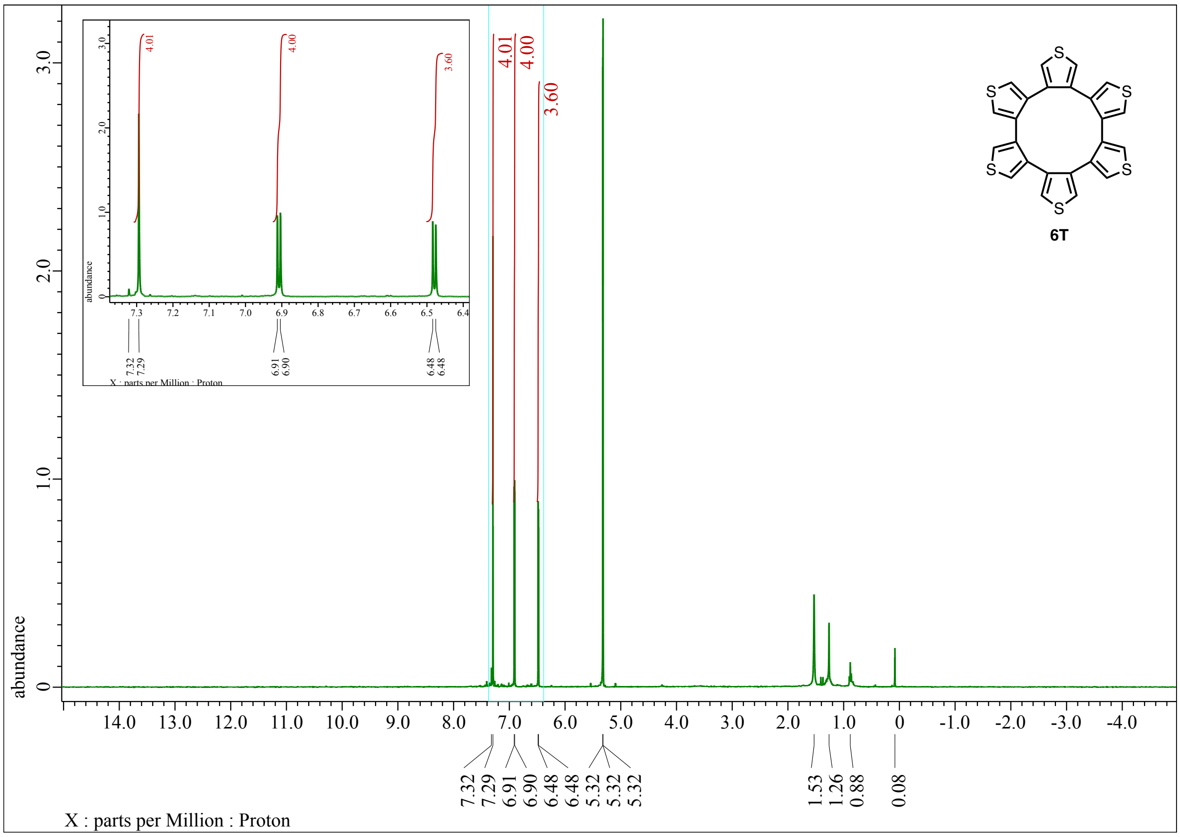

^{1}H NMR spectrum of **6T** (400 MHz, $C_2D_2Cl_4$) at 140 °C

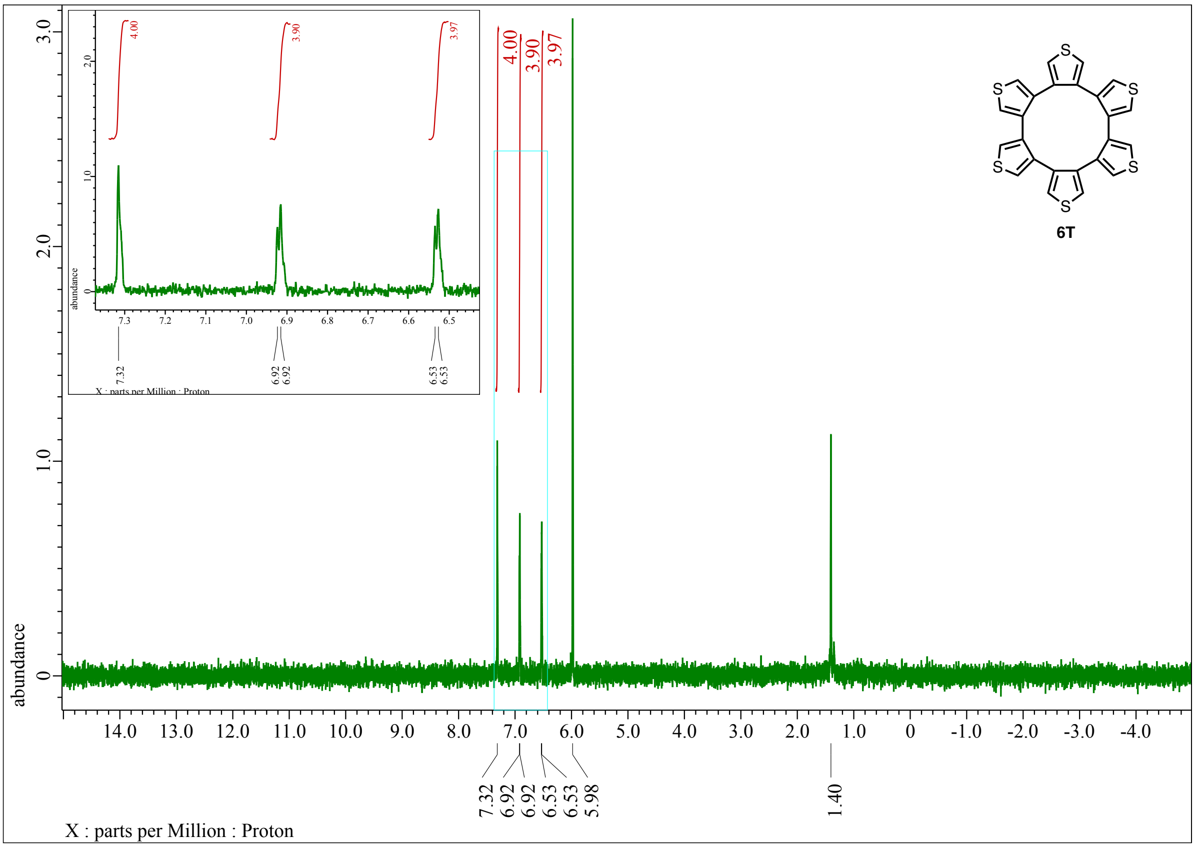

^{13}C NMR spectrum of **6T** (100 MHz, CDCl$_3$)

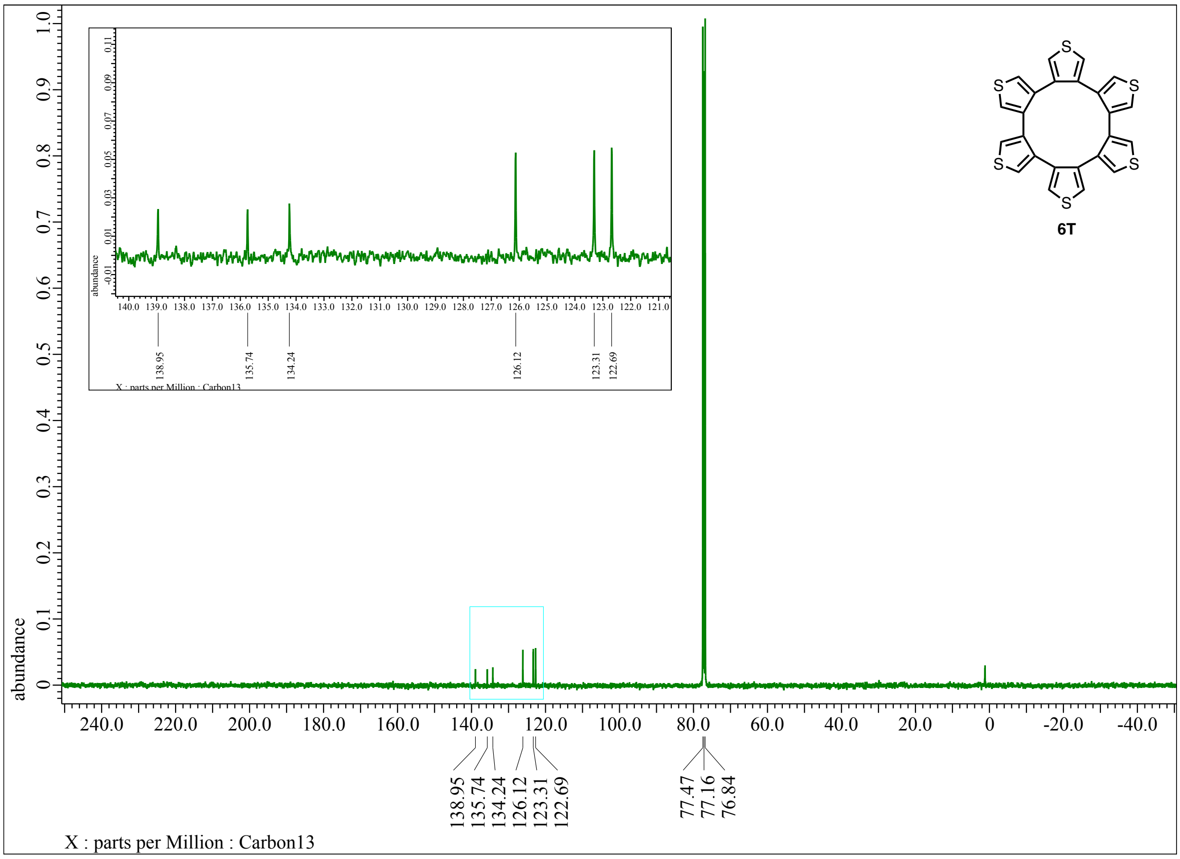

Mass spectrum of **6T** (MALDI-TOF MS)

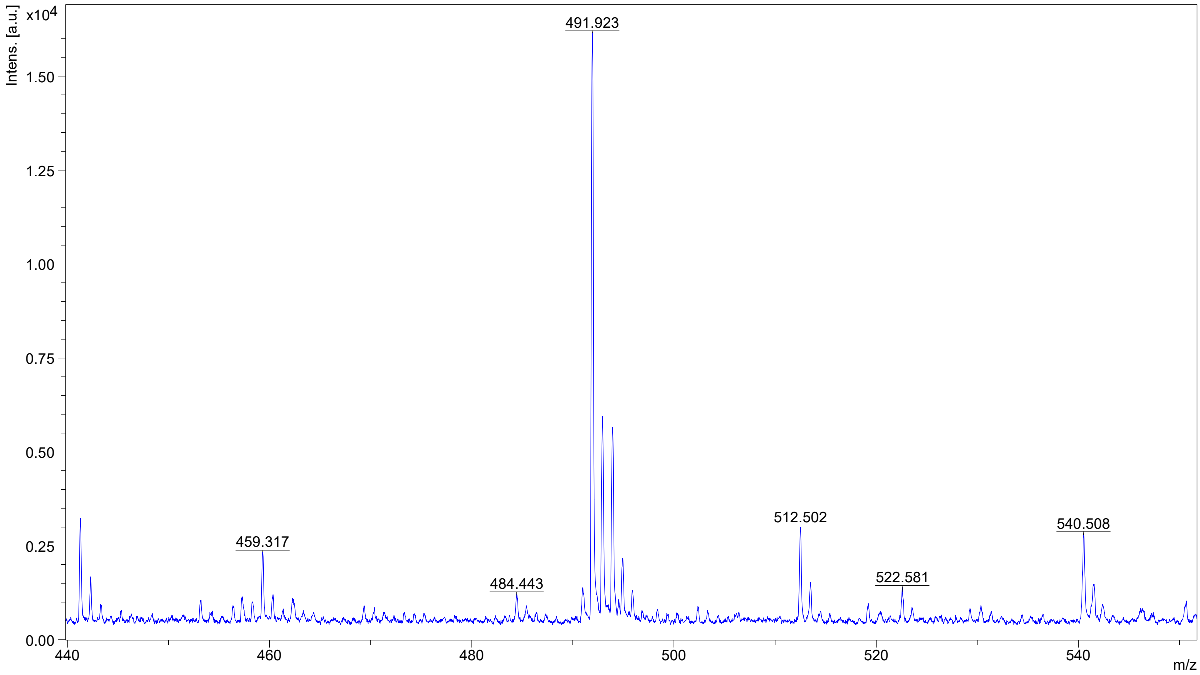

^{1}H NMR spectrum of **4T** (400 MHz, CD_2Cl_2)